Thermal and Hydraulic Characterization of supercritical CO_2 flow in Additively Manufactured Pin-fin Heat Sinks

Ines-Noelly Tano[1], Erfan Rasouli[1], Caton Mande[1], Vinod Narayanan[1], Ziheng Wu[2], Nicholas Lamprinakos[2], Srujana Rao Yarasi[2], Junwon Seo[2], Anthony D. Rollett[2]

[1]University of California, Davis, 2132 Bainer Hall One Shields Avenue, Davis, CA 95616, USA

[2]Carnegie Mellon University, 5000 Forbes Avenue, Pittsburgh, PA 15213, USA

Abstract/Introduction

Compact Heat Exchangers (HX) in supercritical CO_2 (sCO_2) Brayton cycles utilize flow through microscale flow passages. Correlation-based thermofluidic modeling of HXs can be useful in optimizing the design of such HXs. These models rely on accurate pressure drop and heat transfer correlations. In this work, we present experimental results for the development of correlations for one such compact HX based on flow through microscale pin arrays. Existing correlations for pin arrays are based largely on literature in thermal management. Hence, there is need for further performance characterization of sCO_2 flows in such geometries.

The pin array heat sinks in this study are additively manufactured using laser powder bed fusion method out of Haynes 230 powder- a high temperature nickel super alloy. The surface finish and feature dimensions are characterized with optical microscopy. Abrasive flow machining is used for surface roughness treatment of internal passages in the fabricated heat sinks. Thermofluidic experiments are performed with 120 bar sCO_2 that is preheated up to 250 °C prior the heat sink. The sCO_2 mass flow rate supplied to the heat sink results in Reynolds number in the range of 2000 to 8000. Heat transfer and pressure drop results are presented in a non-dimensional form as Nusselt number and friction factor, respectively, and are compared against available correlations in the literature. The experimentally verified design of the heat sink can be used to develop lower uncertainty correlations for use in correlation-based simple HX design models.

Experimental Setup

Pressure drop testing

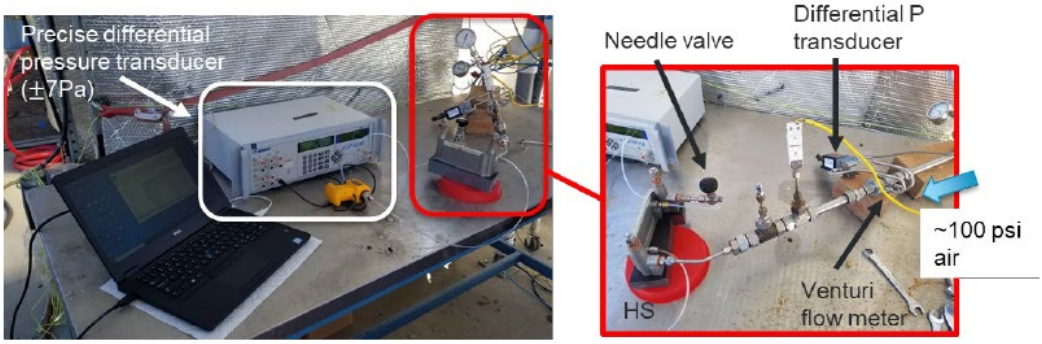

Figure 1. Experimental set-up for pressure drop testing

Pressure drop measurements were performed using an open-loop air facility shown in Figure 1. The heat sinks were 10 cm long and 5 cm in width. To quantify the pressure drop caused only by the pin arrays and not the headers, 1/16 inch NPT ports were used to connect the positive and negative sides of a precise differential pressure transducer (with bias uncertainty of ±7 Pa). Upstream of the heat sink (HS), the incoming airflow passed through a straight section where the line pressure and temperature were recorded, and mass flow rate was measured using a venturi flow meter. Downstream of the HS, a needle valve was placed to regulate the flow rate. All the measurements were recorded continuously throughout the experiments via a LabVIEW program.

Heat transfer testing

Figure 2 shows the experimental setup for heat transfer testing, performed using sCO_2 as the working fluid. The inlet sCO_2 temperature and system pressure in heat transfer testing campaign varied between 70-300 °C and 80-120 bar respectively. The tested sCO_2 flow rates varied between 1- 8 g/s. The heat sink was placed on a heat flux meter consisting of an array of cartridge heaters and thermocouples. The heat transfer coefficient was obtained by a measure of the heat flux, heat sink surface temperature and bulk fluid inlet and exit temperatures for the mass flow rates considered. Data were collected over a range of mass flow rates and analyzed.

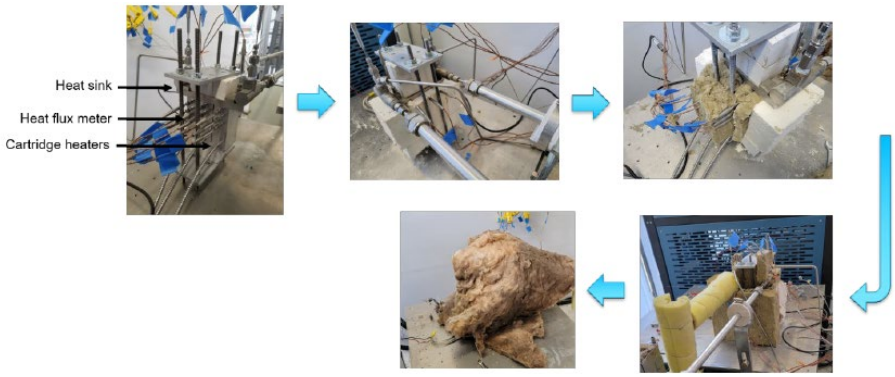

Figure 2. Test section including heat sink, heat flux meter and insulation.

Results

The pin arrays were fabricated in several variants summarized in Table 1. The baseline has a cross section of the pin shaped as half circle-half ellipse to obtain better pin circularity while printing with H230.

Table 1. Design variations of the heat sinks

	Baseline	v1	v2	v3	v4
Design cross-section shape	Half circle Half ellipse	Circle	Half circle Half ellipse	Half circle Half ellipse	Half circle Half ellipse
Design diameter (mm)	1.2	1.2	1.2	1.2	1.2
Printed diameter (mm)	1.1	1.65	1.1	1.1	1.1
Aspect ratio, α	1.64	0.73	2.73	1.64	1.64
Transverse pitch, β_T	2.43	1.49	2.43	3.82	2.43
Longitudinal pitch, β_L	2.11	1.29	2.11	3.31	3.04

The pressure drop variation as function of air mass flow rate is shown on Figure 3a, and the dimensionless equivalent, friction factor variation with Reynolds number is shown on Figure 3b. The Reynolds number was calculated based on minimum cross section area that fluid experienced passing across the pin array. For a given Re number, v1 which has the most flow restriction displays the highest pressure drop. Variant 2 and v3, which are respectively taller and sparser array than the baseline, result in lower pressure drop. The transverse and longitudinal pitches in all the arrays are coupled such that β_L/β_T has a value of 0.86, except in v4 where that value is 1.25. Since the array is sparser than the baseline, the pressure drop at an equivalent Re is lower.

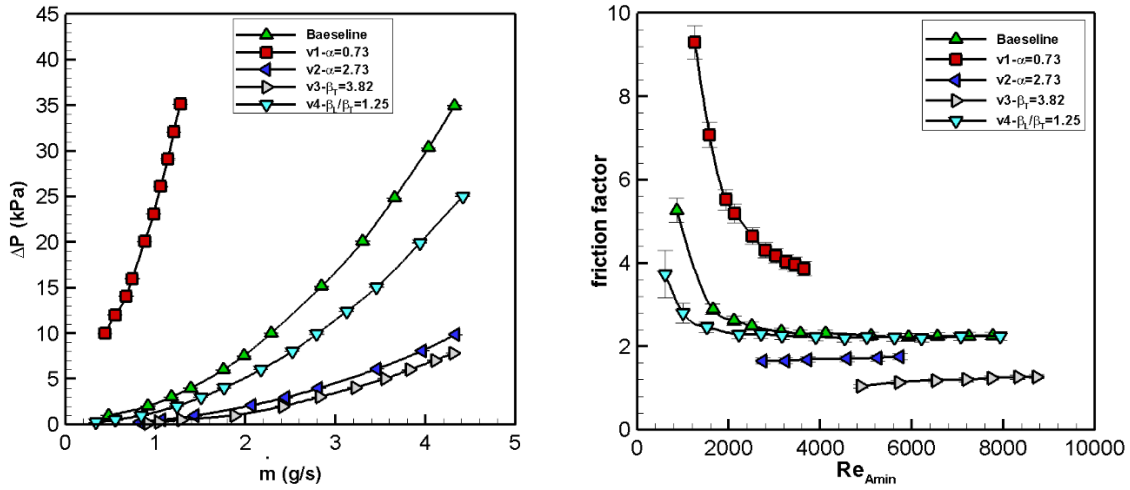

Figure 3. a) Pressure drop as function of mass flow rate, b) Friction factor variation with Reynolds number.

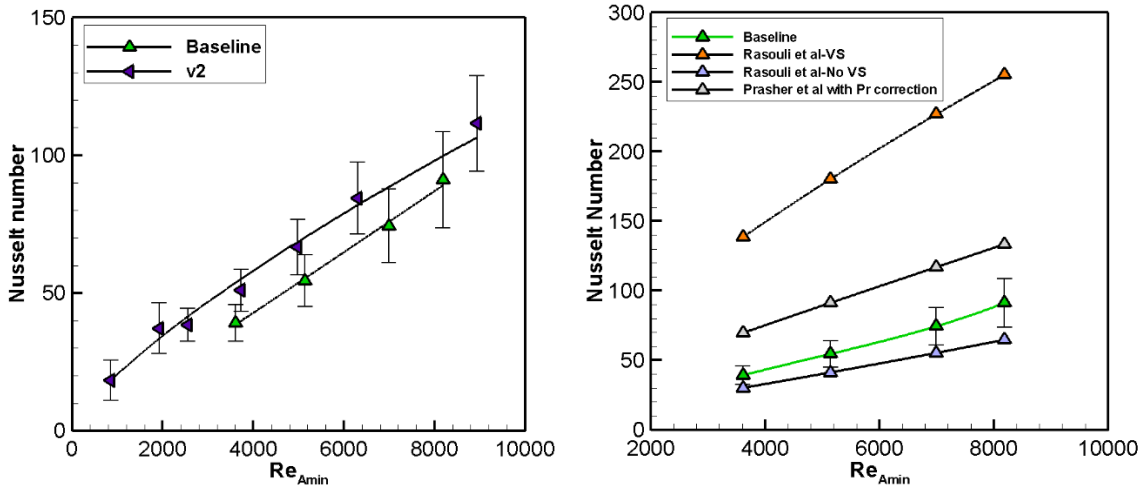

Figure 4. a) Nusselt number variation with Reynolds number, b) Comparison of experimental results against correlations for the baseline pin array.

The Nusselt number results as a function of Re are shown in Figure 4. Also shown in Figure 4b are three correlations from literature- Prasher et al. [1], and a vortex-shedding and non-vortex shedding correlation by Rasouli et al. [2]. The latter correlation was developed in earlier work by using PF-5060 and LN2 flows through diamond-shaped pin fin heat sinks. From Figure 4, the

non-vortex shedding correlation of Rasouli et al. [2] shows the best predictive capability. While the design dimensions of the pin array were designed to induce vortex shedding with aspect ratio and longitudinal pitch greater than unity, and transverse pitch in excess of 2, it is suspected from measurements of analogous heat sinks that the printed dimension transverse with respect to the flow path resulted in a non-vortex shedding condition.

A post-processing step of Abrasive Flow Machining (AFM) was applied in a few heat sinks in an attempt to reduce the surface roughness and study its impact on pressure drop and heat transfer in additively manufactured heat sinks. Table 2 shows a sample of roughness measurements conducted on the internal wall surfaces of two heat sinks and Figure 5 shows optical images of a pin and wall section of a heat sink.

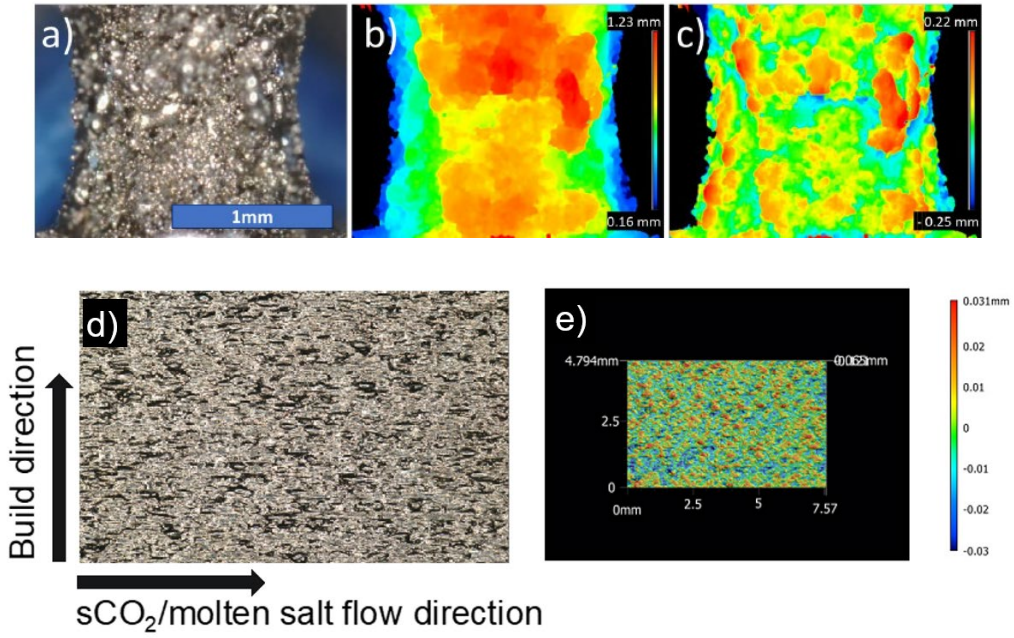

Figure 5. a) Optical image and (b) height map of a bottom surface of a pin obtained by 3D scanner. c) Height map of a flattened surface after surface shape correction, d-e) Roughness profile of vertical wall surface.

Table 2. Comparison of the surface roughness of the internal wall surfaces of two heat sinks.

Heat sink	Surface	Ra (μm)	Rz (μm)	Standard deviation of Ra (μm)	Standard deviation of Rz (μm)
Before AFM	Internal wall	11.8	239.8	1.1	157.7
After AFM	Internal wall	9.5	159.8	1.0	115.6

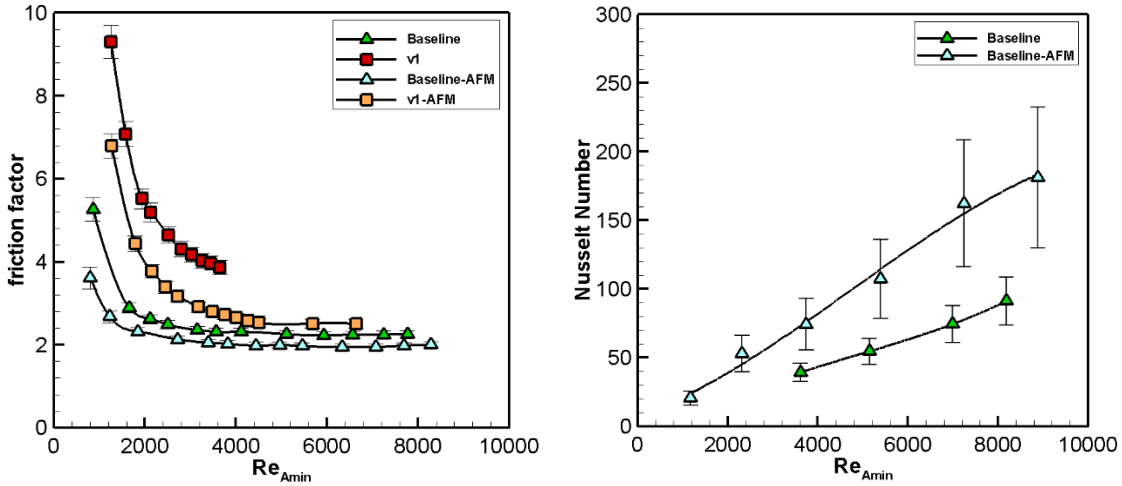

Figure 6. a) Friction factor b) Nusselt number variation with Reynolds number, before and after AFM.

The impact of AFM on pressure non-dimensional pressure drop and heat transfer coefficient is shown in Figure 6a and 6b, respectively. The results obtained show that AFM cause a reduction in surface roughness and an increase in Nusselt number. Efforts are underway to quantify the dimensional changes that might lead to the observed thermohydraulic performance. One plausible explanation for the increase in heat transfer despite the anticipated adverse effect from a roughness reduction is that AFM may remove flow obstructions in channels partially closed at the end of the printing process.

Conclusions

This study showed the impact of parametric variations on heat transfer and pressure drop in additively manufactured heat sinks, as well as potential levers to enhance their thermofluidic performance. A study of the roughness impact was also introduced through testing of pin arrays before and after the abrasive flow machining process. Future work will include gathering more data to develop correlations for pressure drop and heat transfer, with incorporation of the effect of surface roughness.

Acknowledgements

The authors would like to acknowledge the financial support of U.S. Department of Energy's (DOE) Solar Energy Technology Office (SETO) [award # DE-EE0008536] and the Advanced Research Projects Agency-Energy (ARPA-E) [award # DE-AR0001127].

References Cited

1. R. S. Prasher, J. Dirner, J. Y. Chang, A. Myers, D. Chau, D. He, and S. Prstic, "Nusselt Number and Friction Factor of Staggered Arrays of Low Aspect Micropin–fins under Cross Flow for Water as Fluid," J. Heat Transfer, vol. 129, no. 2, pp. 141-153, 2007
2. E. Rasouli, C. Naderi, V. Narayanan, 2018, "Pitch and Aspect Ratios Effects on Single-Phase Heat Transfer through Microscale Pin Fin Heat Sinks", International Journal of Heat and Mass Transfer, Vol. 118, pp. 416-428.